Shape resonances in the photoionization of cyanogen

D. L. Lynch, S. N. Dixit, and V. McKoy
Arthur Amos Noyes Laboratory of Chemical Physics,[a] *California Institute of Technology, Pasadena, California 91125*

(Received 18 September 1985; accepted 27 January 1986)

We have studied the photoionization cross sections and photoelectron asymmetry parameters for ionization of the $1\pi_g$ ($X\,^2\Pi_g$), $5\sigma_g$ ($A\,^2\Sigma_g^+$), and $4\sigma_u$ ($B\,^2\Sigma_u^+$) levels of cyanogen using frozen-core Hartree–Fock photoelectron continuum orbitals. The main purpose of these studies has been to extend our understanding of the dynamics of shape resonances from earlier studies of diatomic and smaller polyatomic molecules to a larger polyatomic system. The results do, in fact, reveal a rich shape resonant structure in the electronic continuum of this polyatomic system. There is a low-energy σ_u resonance which, as expected, is the C–C analog of the $l = 3$ shape resonance seen in $N_2(3\sigma_g^{-1})$ and several other diatomics. In contrast to this diatomic-like behavior, the presence of the two CN groups in C_2N_2 results in a second σ_u and a σ_g resonance corresponding to linear combinations of a $l = 3$ shape resonance localized on the CN sites. Moreover, our results also show a pronounced shape resonant behavior in the π_u continuum, which, to our knowledge, has not been seen in smaller molecules.

I. INTRODUCTION

Shape resonances play a central role in studies of the dynamics of molecular photoionization. They give rise to several distinct features in the photoionization of molecules such as an enhancement of the cross sections, a pronounced influence on the angular distributions of photoelectrons, and non-Franck–Condon effects in vibrationally resolved spectra.[1,2] These shape resonances are quasibound states formed by the trapping of the photoelectron by the centrifugal barrier of the molecular force field. A study of these resonant features naturally provides significant physical insight into the underlying photoionization process.

The effects of shape resonances and autoionizing features have been studied in many molecules over a wide range of photon energies using synchrotron radiation. These systems include, among others,[3] N_2,[4] CO,[5] CO_2,[6] CS_2,[7] and C_2H_2.[8] The availability of such experimental data and the difficulties associated with theoretical studies of molecular photoionization have stimulated the development of various approaches to the calculation of these photoionization cross sections. These approaches include the Stieltjes moment theory method which avoids the need for the direct solution of the collision equations by extracting photoionization cross sections from spectral moments of the oscillator strength distribution,[9] the continuum multiple scattering model in which the molecular potential is approximated so that the continuum equations can be readily solved,[10] and several methods for the direct solution of the Hartree–Fock equations for the photoelectron continuum orbitals.[11–15] These experimental and related theoretical studies have served to clarify many important features such as the positions and symmetries of shape resonances in several diatomic molecules including N_2,[4,14,16–18] CO,[5,16,19–21] O_2,[1,22,23] and NO,[24–26] and in polyatomic molecules, e.g., CO_2,[6,27,28] CS_2,[7,29] and C_2H_2.[8,30,31] The results for CO_2[6,28] and C_2H_2[8,31] have already shown that resonance features in the photoionization of polyatomic molecules can behave very differently from what could be expected on the basis of results for simple diatomic molecules. Our understanding of the dynamics of shape and autoionizing resonances would clearly benefit from an extension of current studies to larger molecular systems.

In this paper we report the results of studies of the photoionization cross sections and photoelectron asymmetry parameters for ionization of the $1\pi_g$ ($X\,^2\Pi_g$), $5\sigma_g$ ($A\,^2\Sigma_g^+$), and $4\sigma_u$ ($B\,^2\Sigma_u^+$) levels of cyanogen, C_2N_2. We chose this system primarily for the interesting shape resonant structure which it can be expected to exhibit. Specifically, there is the possibility of shape resonant trapping arising from both the CN components of the molecule and from the C–C bond itself. Moreover, the presence of two CN groups should result in resonances corresponding to the in-phase and out-of-phase combinations of these trapping sites. These resonances, which are derived from the C≡N analog of the well-known σ shape resonances in diatomic molecules, should occur in both the σ_g and σ_u continua. We can hence expect two shape resonances in the σ_u continuum, the lower energy one arising from the C–C bond and the higher one arising from the CN groups, and a single shape resonance in the σ_g continuum.

These σ_u and σ_g shape resonant features in the photoionization of the $1\pi_g$, $5\sigma_g$, $4\sigma_u$, and $1\pi_u$ levels of C_2N_2 have been discussed previously by Holland *et al.*[32] and by Kreile *et al.*[33] The synchrotron radiation studies[32] extended from threshold to a photon energy of 24 eV and hence, as we will see, did not include the energy region where the σ_u and σ_g CN-related resonances occur. However, our results show that the pronounced dip in the photoelectron asymmetry parameter curve for the $5\sigma_g$ level occurring at a photon energy of 16.5 eV is due to the σ_u C–C shape resonance. On the other hand, the similar behavior of the asymmetry parameters for the $1\pi_g$ level in the same energy region[32] is not due to this shape resonance and is almost certainly an autoionization feature.[32] The Ne I, He I, and Ne II line source measurements of the vibrationally resolved asymmetry param-

[a] Contribution No. 7218.

 0021-9606/86/105504-09$02.10

eters also show strong evidence of the C–C σ_u resonance in photoionization of the $5\sigma_g$ orbital.[33] Studies of these photoionization cross sections using the multiple scattering model predict both a high and a low energy shape resonance in the σ_u continuum, a σ_g shape resonance, and a very pronounced shape resonance in the π_g continuum.[33]

A summary of our results for the shape resonant behavior in the electronic continua of $C_2N_2^+$ is as follows. The C–C σ_u shape resonance occurs at a photoelectron kinetic energy of about 2.5 eV while the σ_g and σ_u shape resonances associated with the CN groups are seen at kinetic energies of 18 and 27 eV, respectively, or a σ_g–σ_u splitting of about 9 eV. However, we also predict a broad shape resonance in the π_u continuum with an onset just below a photon energy of 26 eV. This shape resonance has not been previously identified. The measured photoelectron asymmetry parameters, β, do show a pronounced vibrational state dependence at a photon energy of 26.91 eV with values of 0.52 and 1.09 for $\nu_1 = 0$ and 1, respectively, in the symmetric C≡N stretching mode.[33] Our calculated fixed-nuclei β value of about 1.1 at this energy is in poor agreement with these measured β's since the photoelectron spectra at this energy and below[32,34] show that the intensity of the $\nu_1 = 1$ member of this $^2\Sigma_g^+ (5\sigma_g^{-1})$ band is much smaller than that of the $\nu_1 = 0$ member and hence the fixed-nuclei result can be expected to be close to $\beta(\nu_1 = 0)$. These results will be discussed further in Sec. III B. With this π_u shape resonance and the two resonances in the σ_u continuum, photoionization out of the $5\sigma_g$ orbital shows three resonance features. The actual influence of a shape resonance in a specific continuum on the vibrationally unresolved cross sections is also seen to vary significantly from channel to channel. For example, while the $k\pi_u$ shape resonance is pronounced in the cross sections for photoionization out of the $5\sigma_g$ level, we see essentially no evidence of this shape resonance in the vibrationally unresolved $1\pi_g$ cross sections. This shape resonance is, however, seen in the eigenphase sums in both channels. Eigenphase sums are clearly very useful in identifying the presence and nature of these shape resonances. In contrast to the results of the continuum miltiple scattering model[33] we do not see a shape resonance in the $4\sigma_u \rightarrow k\pi_g$ cross sections. Furthermore, the photoionization cross sections in some channels can be affected substantially by electron correlation. For example, in the Hartree–Fock approximation, a discrete level can be incorrectly forced into the continuum, or too close to threshold, resulting in spurious behavior of the cross sections. For cyanogen, this occurs in photoionization of the $1\pi_g$ level into the $k\pi_u$ and $k\sigma_u$ continua. These results suggest that vibrationally resolved measurements of the photoionization cross sections and asymmetry parameters for cyanogen will provide a rich source of dynamical information on molecular photoionization.

An outline of the paper is as follows. In Sec. II we give a brief discussion of the method used to obtain the Hartree–Fock electronic continuum orbitals needed in these studies along with several relevant computational details. In Sec. III we present our calculated photoionization cross sections and photoelectron asymmetry parameters for the $1\pi_g$, $5\sigma_g$, and $4\sigma_u$ levels of C_2N_2 and compare these results with available experimental data and with the results of other calculations.[33]

II. METHOD

The rotationally unresolved, fixed-nuclei photoionization cross section is given by

$$\sigma(R) = \frac{4\pi^2\omega}{3c} |\langle \Psi_i(\mathbf{r},R) | \mu | \Psi_f(\mathbf{r},R) \rangle|^2, \quad (1)$$

where μ is the dipole moment operator and ω is the photon frequency. In Eq. (1) Ψ_i represents the initial state of the molecule with N bound electrons and Ψ_f the final state with a photoelectron in the electronic continuum. The representation of Ψ_f requires a set of continuum orbitals describing the motion of the photoelectron in the nonlocal, nonspherical potential field of the molecular ion. In these studies we will use the Hartree–Fock continuum orbitals of the molecular ion which satisfy the one-electron Schrödinger equation (in atomic units)

$$[-\tfrac{1}{2}\nabla^2 + V_{N-1}(\mathbf{r},R) - (k^2/2)]\phi_{\mathbf{k}}(\mathbf{r},R) = 0, \quad (2)$$

where $k^2/2$ is the photoelectron kinetic energy, V_{N-1} is the Hartree–Fock (static-exchange) potential of the ion, and $\phi_{\mathbf{k}}$ satisfies the appropriate boundary conditions. We also use the frozen-core approximation and hence assume that V_{N-1} is determined by the core orbitals of the neutral molecule.

The nonspherical and nonlocal character of molecular potentials introduces several complications into the solution of Eq. (2) for continuum orbitals. In our studies we will use the Schwinger variational procedure to solve Eq. (2) for the continuum orbitals[14,35] needed to obtain the photoionization cross sections and angular distributions of the photoelectron. Other techniques have also been developed for the direct solution of the Hartree–Fock equations for these molecular continuum orbitals.[3,11–15] Results to date have shown that there can be significant advantages in utilizing Hartree–Fock continuum orbitals explicitly in molecular photoionization studies, particularly in regions of shape resonances.[3]

We solve Eq. (2) by working with the integral form of this equation, i.e.,

$$\phi_{\mathbf{k}} = \phi_{\mathbf{k}}^c + G_c^{(-)} V \phi_{\mathbf{k}}, \quad (3)$$

where $\phi_{\mathbf{k}}^c$ is the pure Coulomb scattering function, V is the molecular ion potential with the Coulomb component removed, and $G_c^{(-)}$ is the Coulomb Green's function with incoming-wave boundary conditions,

$$V = V_{N-1} + (1/r), \quad (4a)$$

$$G_c^{(-)} = 2[\nabla^2 + (2/r) + k^2 - i\epsilon]^{-1}. \quad (4b)$$

The continuum orbital $\phi_{\mathbf{k}}(\mathbf{r})$ can be expanded in terms of spherical harmonics of $\Omega_{\hat{k}}$, the direction of $\mathbf{k}$, as

$$\phi_{\mathbf{k}}(\mathbf{r}) = \left(\frac{2}{\pi}\right)^{1/2} \sum_{lm} \frac{i^l}{k} \phi_{klm}(\mathbf{r})\, Y_{lm}^*(\Omega_{\hat{k}}), \quad (5)$$

where $\phi_{klm}(\mathbf{r})$ is a partial wave scattering function. Each ϕ_{klm} satisfies its own Lippmann–Schwinger equation, i.e.,

$$\phi_{klm} = \phi_{klm}^c + G_c^{(-)} V \phi_{klm}. \quad (6)$$

We first obtain an approximate solution of Eq. (6) for ϕ_{klm} assuming a separable approximation for the potential V of the form

$$V(\mathbf{r},\mathbf{r}') \simeq V^s(\mathbf{r},\mathbf{r}') = \sum_{i,j} \langle \mathbf{r}|V|\alpha_i\rangle (V^{-1})_{ij} \langle \alpha_j|V|\mathbf{r}'\rangle , \quad (7)$$

where the matrix $(V^{-1})_{ij}$ is the inverse of the matrix with elements $V_{ij} = \langle \alpha_i|V|\alpha_j\rangle$. With the approximate potential of the form of Eq. (7), the solutions of the integral equation, Eq. (6), can be written

$$\phi^{(0)}_{klm}(\mathbf{r}) = \phi^c_{klm} + \sum_{i,j} \langle \mathbf{r}|G_c^{(-)}V|\alpha_i\rangle \times (D^{-1})_{ij} \langle \alpha_j|V|\phi^c_{klm}\rangle , \quad (8)$$

where the matrix $(D^{-1})_{ij}$ is the inverse of the matrix

$$D_{ij} = \langle \alpha_i|V - VG_c^{(-)}V|\alpha_j\rangle . \quad (9)$$

The use of a separable potential of the form of Eq. (7) in Eq. (6) to obtain solutions of the form of Eq. (8) can be shown to be equivalent to using the basis functions $\alpha_i(\mathbf{r})$ in the Schwinger variational principle for collisions.[36] The function $\alpha_i(\mathbf{r})$ can be chosen to be entirely discrete basis functions such as Cartesian Gaussian[37] or spherical Gaussian[28] functions. We note that with discrete basis functions alone these approximate solutions $\phi^{(0)}_{klm}$ satisfy scattering boundary conditions. These discrete basis functions have been used successfully in electronic structure calculations[37] and should be very effective in representing the multicenter nature of the scattering wave function and molecular potential in the near-molecular region. With adequate basis sets the continuum solutions of Eq. (8) already provide quantitatively reliable, photoionization cross sections[2,3] which, moreover, can be shown to be variationally stable at the Hartree–Fock level.[38] Although we have developed an iterative procedure for obtaining the converged solutions of Eq. (6),[35] in these studies the cross sections were generally determined using the approximate solutions $\phi^{(0)}_{klm}$ obtained with an adequate expansion basis in Eq. (8). For photoionization of the $5\sigma_g$ level, we did, however, explicitly verify that the cross sections changed only slightly with iteration. For example, at the peak of the shape resonant $5\sigma_g - k\sigma_u$ partial channel (17.5 eV) the length form of cross section changes from 8.04 to 8.01 Mb upon iterating.

For the initial state we have used the SCF Slater basis wave function of McLean and Yoshimine[39] with C–C and C–N bond lengths of 2.608 and 2.186 a.u., respectively. All the matrix elements and functions arising in the solution of Eq. (8) were evaluated using single-center expansions. Details of these numerical procedures have been discussed previously.[14] The single-center expansions are made about the molecular center and the expansion parameters were based on the experience of earlier studies of CO_2.[28] These parameters are defined in Ref. 28 and are as follows:

(i) $l_m = l_s^{ex} = l_i^{dir} = 59$,

(ii) $l_m^{ex} = 40$,

(iii) $\lambda_m^{dir} = 118$,

(iv) $l_i^{ex} = 58(1\sigma_g), 22(2\sigma_g), 26(3\sigma_g), 18(4\sigma_g), 20(5\sigma_g), 59(1\sigma_u), 23(2\sigma_u), 29(3\sigma_u), 21(4\sigma_u), 17(1\pi_u)$, and $16(1\pi_g)$,

(v) $l_p = 10$.

Based on earlier convergence studies[14,28] these values of the expansion parameters should provide cross sections which are within a few percent of the converged values. The above values of l_i^{ex} correspond to having normalized the molecular orbital expansions to better than 0.99. For example, extending l_m^{ex} to 59 changes the peak of the $5\sigma_g \rightarrow k\sigma_u$ cross section at 17.5 eV by less than 1%.

For the expansion basis in Eq. (7) we use spherical Gaussian functions which are defined by

$$\chi(\mathbf{r}) = N|\mathbf{r}-\mathbf{A}|^l \exp(-\alpha|\mathbf{r}-\mathbf{A}|^2) Y_{lm}(\Omega_{\mathbf{r}-\mathbf{A}}) . \quad (10)$$

The basis sets for the various ionization channels are given in Table I.

III. RESULTS AND DISCUSSION

A. Photoionization cross sections for the $X\,^2\Pi_g(1\pi_g^{-1})$ ion

Figure 1 shows the contributions of the σ_u, π_u, and δ_u continua to the photoionization cross section for the $1\pi_g$ level. In this figure we have assumed the experimental value of 13.36 eV for the ionization potential of this state.[32] The $k\pi_u$ and $k\sigma_u$ cross sections show a very sharp and conspicuous increase near threshold which is probably unphysical and due to the occurrence of the $1\pi_g^3 2\pi_u(^1\Sigma_u^+)$ and $1\pi_g^3 5\sigma_u(^1\Pi_u)$ excitations too close to threshold in the Hartree–Fock approximation. In fact, in Hartree–Fock calculations of the spectrum of C_2N_2, Bell[40] obtained excitation energies of 12.76 and 12.6 eV, respectively, for the $1\pi_g \rightarrow 2\pi_u$ and $1\pi_g \rightarrow 5\sigma_u$ transitions. These values are considerably larger than the excitation energies tentatively assigned to these transitions in the vacuum UV spectrum and are quite close to the calculated ionization potential of 13.08 eV.[40] To assess the influence on the cross sections of these discrete transitions which may be spuriously close to threshold, we have calculated the corresponding cross sections using $k\pi_u$ and $k\sigma_u$ continuum orbitals orthogonalized to the $2\pi_u$ and $5\sigma_u$ virtual orbitals of the Hartree–Fock calculation. We have shown that this very approximate procedure provides a useful estimate of the photoionization cross section which would result if these discrete transitions were further removed from threshold and closer to their correct locations.[14] The resulting cross sections in the dipole length approximation are shown in Fig. 2 and are seen to be very strongly influenced by this orthogonalization.

Figure 3 shows the eigenphase sums for the σ_u, π_u, and δ_u continua of the $X\,^2\Pi_g(1\pi_g^{-1})$ ion. These eigenphase sums show clear evidence of two shape resonances in the σ_u continuum and one in the π_u continuum. However, the σ_u and π_u cross sections of Fig. 1 do not show any clearly related resonant structure. On the other hand, we will see that these three shape resonances appear very distinctly in both the corresponding eigenphase sums and cross sections for ionization out of the $5\sigma_g$ level. In comparison, the $k\delta_u$ eigenphase sums and cross section are characteristically nonresonant.

In Fig. 4 we show our calculated total photoionization cross sections for the $1\pi_g$ orbital using both the length and velocity forms of the dipole transition moment. The significant differences between these length and velocity cross sec-

TABLE I. Basis sets used for σ, π, and δ continuum solutions.

Channel	Center	l	m	Exponent
$4\sigma_u \rightarrow k\sigma_g$	N	0	0	16,8,4,2,1,0.5
		1	0	8,4,2,1,0.5
		2	0	2,1,0.5
	C	0	0	16,8,4,2,1,0.5
		1	0	8,4,2,1,0.5
		2	0	2,1,0.5
	CM[a]	0	0	1,0.5
		2	0	1.0
		4	0	0.5
$4\sigma_u \rightarrow k\pi_g$	N	1	1	8,4,2,1,0.5
		2	1	8,4,2,1,0.5
	C	1	1	8,4,2,1,0.5
		2	1	8,4,2,1,0.5
	CM	2	1	1,0.5,0.1
		4	1	1,0.5,0.1
$1\pi_g \rightarrow k\sigma_u$	N	0	0	10,4,2,1,0.5,0.1
		1	0	4,2,1,0.5,0.1
		2	0	2,1,0.5,0.1
	C	0	0	10,4,2,1,0.5,0.1
		1	0	4,2,1,0.5,0.1
		2	0	2,1,0.5,0.1
	CM	1	0	1,0.5,0.1
		3	0	0.5,0.1
		5	0	0.5,0.1
$1\pi_g \rightarrow k\pi_u$	N	1	1	8,4,2,1,0.5,0.1
		2	1	8,4,2,1,0.5,0.1
	C	1	1	8,4,2,1,0.5,0.1
		2	1	2,1,0.5,0.1
	CM	1	1	1,0.5,0.1
		3	1	1,0.1
		5	1	0.5,0.1
$1\pi_g \rightarrow k\delta_u$	N	2	2	8,4,2,1,0.5,0.1
		3	2	2,1,0.5,0.1
	C	2	2	8,4,2,1,0.5,0.1
		3	2	2,1,0.5,0.1
	CM	3	2	1,0.1
		5	2	0.5,0.1
$5\sigma_g \rightarrow k\sigma_u$	N	0	0	8,4,2,1,0.5
		1	0	8,4,2,1,0.5
		2	0	2,1,0.5
	C	0	0	8,4,2,1,0.5
		1	0	8,4,2,1,0.5
		2	0	2,1,0.5
	CM	1	0	1,0.5
		3	0	1.0
		5	0	0.5
$5\sigma_g \rightarrow k\pi_u$	N	1	1	8,4,2,1,0.5
		2	1	8,4,2,1,0.5
	C	1	1	8,4,2,1,0.5
		2	1	2,1,0.5
	CM	1	1	1,0.5
		3	1	1.0
		5	1	0.5

[a] CM = center of mass.

tions arise primarily from the neglect of electron correlation effects.[14] It is these correlation effects which must be included so as to move the discrete $1\pi_g^3 5\sigma_u$ and $1\pi_g^3 2\pi_u$ states further away from threshold and closer to their correct positions. For comparison, we also show the cross sections obtained using the $k\sigma_u$ and $k\pi_u$ continuum orbitals which have been orthogonalized to the $5\sigma_u$ and $2\pi_u$ virtual orbitals. The effects of this orthogonalization are probably exaggerated due to the very approximate basis of this procedure for reproducing the actual effects of electron correlation.

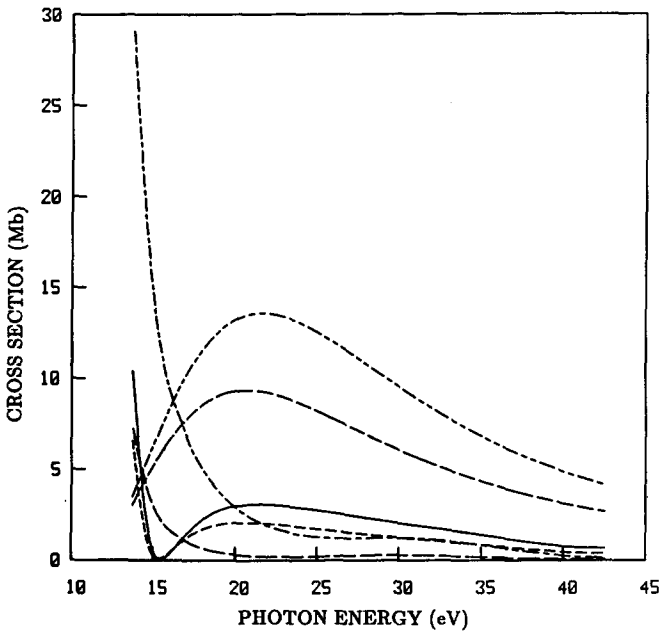

FIG. 1. The $1\pi_g \rightarrow k\sigma_u$, $k\pi_u$, and $k\delta_u$ partial channel photoionization cross sections for C_2N_2: $1\pi_g \rightarrow k\sigma_u$, — (length) and --- (velocity); $1\pi_g \rightarrow k\pi_u$, – – – (length) and – – (velocity); $1\pi_g \rightarrow k\delta_u$, – – – – (length) and – – – – – (velocity).

Finally, we compare our calculated cross sections with those of the continuum multiple scattering model.[33] Although not shown in this figure, the σ_u and δ_u components of our calculated cross sections behave very differently near threshold from those of the multiple scattering model. Whereas our calculated σ_u and δ_u cross sections decrease and increase, respectively, towards threshold, those of the multiple scattering model behave just the other way. No measurements of these cross sections have been reported.

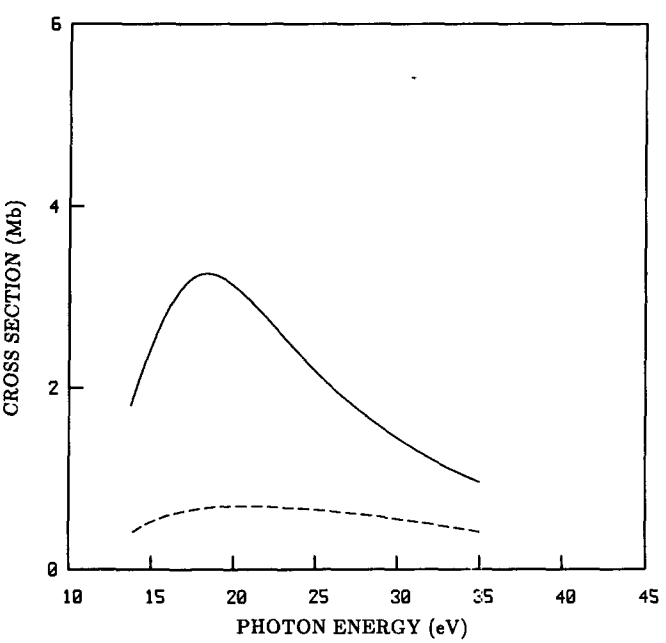

FIG. 2. The $1\pi_g \rightarrow k\sigma_u$ and $k\pi_u$ partial channel cross sections with the continuum $k\sigma_u$ and $k\pi_u$ wave functions orthogonalized to the $5\sigma_u$ and $2\pi_u$ orbitals, respectively: $1\pi_g \rightarrow k\sigma_u$, —; $1\pi_g \rightarrow k\pi_u$, ---.

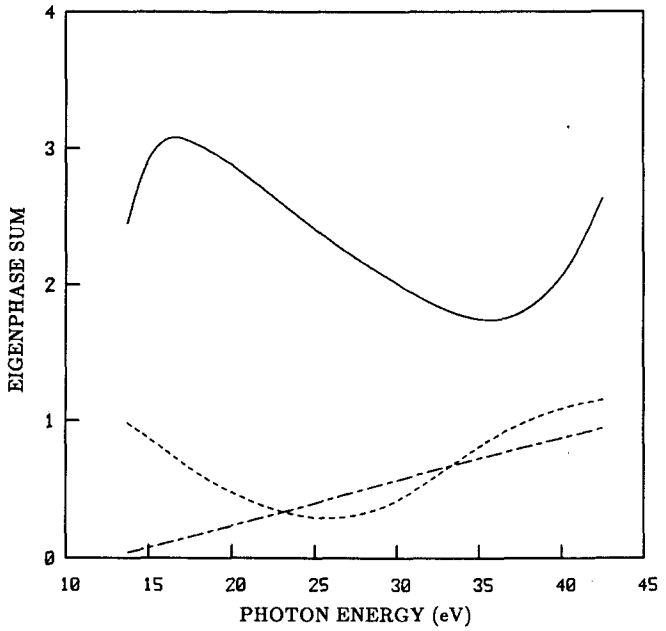

FIG. 3. Eigenphase sums for the $1\pi_g \rightarrow k\sigma_u$ (—), $1\pi_g \rightarrow k\pi_u$ (---), and $1\pi_g \rightarrow k\delta_u$ (- - -) components.

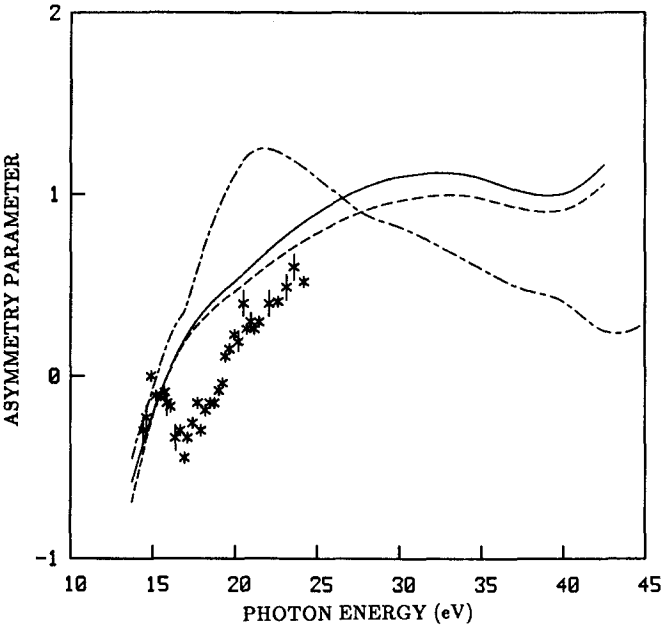

FIG. 5. Photoelectron asymmetry parameters for the $X\,^2\Pi_g$ state: present results, — (length) and --- (velocity); multiple scattering results, - - - (Ref. 33); experimental results ($v = 0$), × (Ref. 32).

Figure 5 shows the calculated photoelectron asymmetry parameter for the $1\pi_g$ level along with the measured values of Holland *et al.*[32] for the $v = 0$ level of the ion. The calculated asymmetry parameters do not show the pronounced resonance structure seen in the experimental data around 17 eV. This structure is almost certainly due to autoionization, e.g., the $4\sigma_g \rightarrow 2\pi_u$ transition,[32] which is not included in these Hartree–Fock continuum calculations. Again, the vibrationally unresolved photoelectron asymmetry parameters show no evidence of the shape resonances suggested by the behavior of the σ_u and π_u eigenphase sums of Fig. 3. However, it is possible that the non-Franck–Condon behavior of the measured vibrational branching ratios for the $v = 0$, 1, 2, and 3 levels below 15.5 eV[32] could be due to the lower energy σ_u shape resonance. Finally, the asymmetry parameters of Kreile *et al.*[33] obtained using the multiple scattering model are shown in Fig. 5. Above 18 eV these asymmetry parameters differ significantly from those of the present Hartree–Fock studies. These differences are much more significant than we have seen in the photoelectron asymmetry parameters predicted by these two methods for other molecules, e.g., N_2[14] and CO_2.[28]

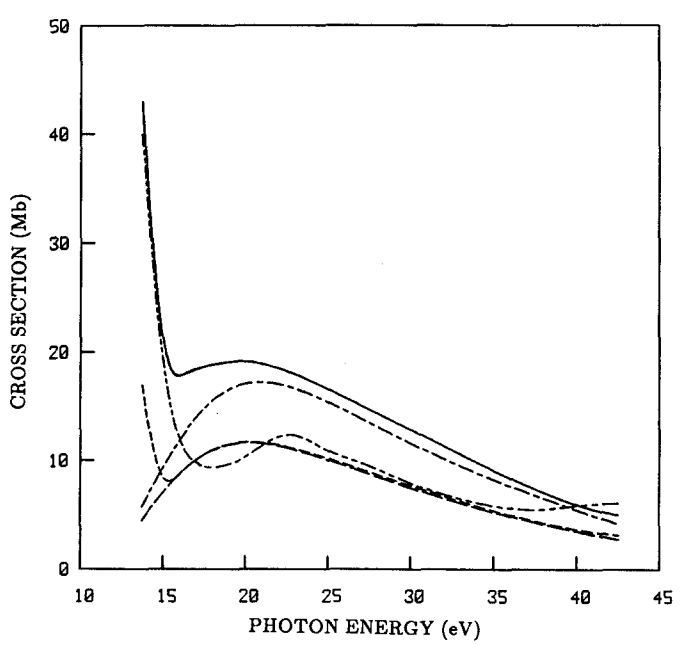

FIG. 4. Calculated cross sections for the $X\,^2\Pi_g$ state of $C_2N_2^+$: present results, — (length) and --- (velocity); present results with the orthogonalized continua, - - - (length) and – – (velocity); multiple scattering model, - - - - (Ref. 33).

B. The $A\,^2\Sigma_g^+ (5\sigma_g^{-1})$ ion

Figure 6 shows our calculated cross sections for photoionization of the $5\sigma_g$ level along with the individual contributions of the σ_u and π_u continua while Fig. 7 gives the eigenphase sums for these two continua. In these figures and in Fig. 8 we assume an ionization potential of 14.49 eV.

These results reveal a rich and interesting shape resonance structure. The σ_u continuum shows both a low and a high energy shape resonance at photon energies of about 17 and 42 eV, or photoelectron kinetic energies of 2.5 and 27.5 eV, respectively. The π_u continuum also shows a shape resonance with a peak position around 33 eV. The behavior of the eigenphase sums associated with these resonances is shown in Fig. 7. The σ_u shape resonance at 2.5 eV into the continuum is the C–C analog of the well-known σ_u ($l = 3$) shape resonance in $N_2(3\sigma_g^{-1})$ which occurs at a kinetic energy of about 15 eV in that system. The origin and character of this shape resonance has been discussed previously.[32,33] Its occurrence at kinetic energies of 2.5 and 15 eV in C_2N_2 and N_2, respectively, is consistent with the much larger C–C bond distance in C_2N_2 (2.608 a.u.) than the N_2 bond distance (2.068 a.u.). These two σ_u shape resonances have also

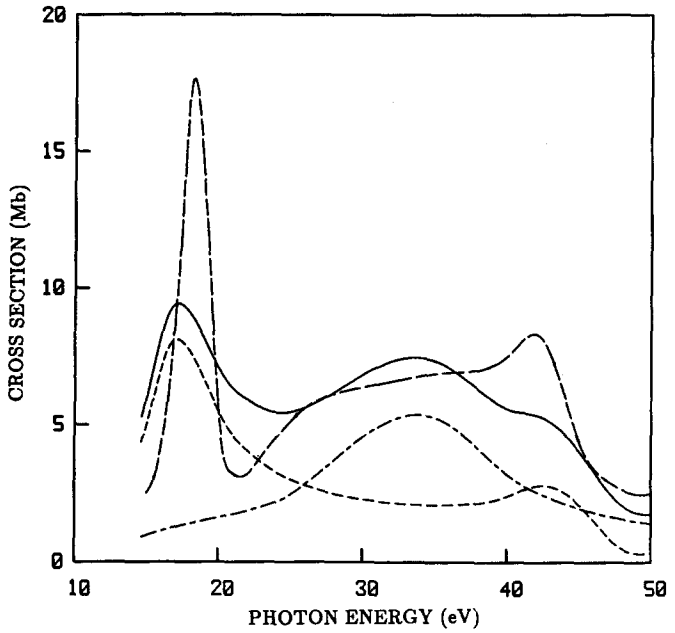

FIG. 6. Photoionization cross sections for the $A\,^2\Sigma_g^+$ state of $C_2N_2^+$: present results (length), — (total), --- ($5\sigma_g \rightarrow k\sigma_u$), and - - - ($5\sigma_g \rightarrow k\pi_u$); multiple scattering results, - - - - (total, Ref. 33).

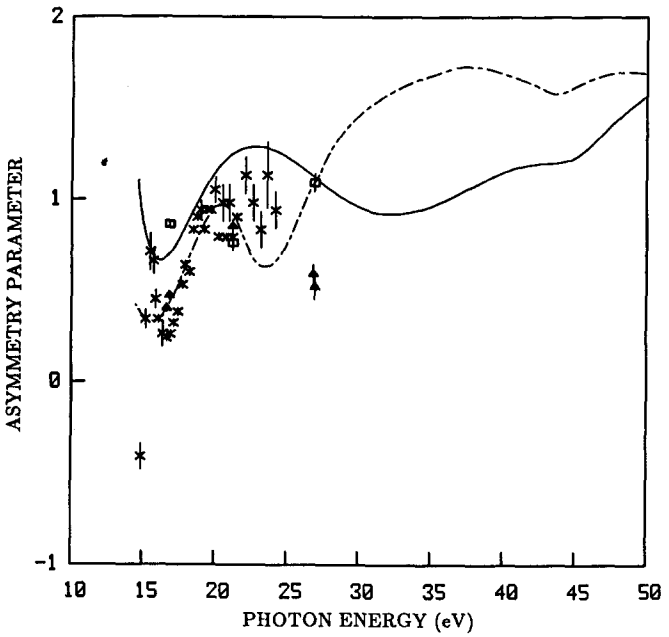

FIG. 8. Asymmetry parameter for the $A\,^2\Sigma_g^+$ state: present results (length) (—); multiple scattering results of Ref. 33 (- - -); experimental results ($v = 0$) of Ref. 32 ($\times$); experimental results of Ref. 33, $\triangle$ ($v_1 = v_2 = 0$) and $\square$ ($v_1 = 1$, $v_2 = 0$).

been seen at around the same energies in the calculated cross sections of the multiple scattering model.[33] However, the peak value of the cross section of the multiple scattering model for the lower energy resonance is about twice as large as that of the present studies while the resonance itself is much narrower. This same trend has been observed in other systems.[28,41]

The K matrices associated with the σ_u shape resonance around 42 eV show significant mixing among the $l = 3$, 5, and 7 partial waves, suggesting that the photoelectron wave function has significant amplitude in the region of the C≡N subgroup. As suggested by Holland *et al.*,[32] this amplitude on the C≡N subgroup is very probably due to the $\sigma(l = 3)$ shape resonance localized in that region of the molecule. This higher energy shape resonance is then just the σ_u combination of these CN localized shape resonances.[32] As we will see shortly, there is also an associated σ_g shape resonance at lower energy. The second σ_u shape resonance does not lead to a very substantial enhancement of the cross section. Its resonant nature, however, is clear from the behavior of the eigenphase sum of Fig. 7.

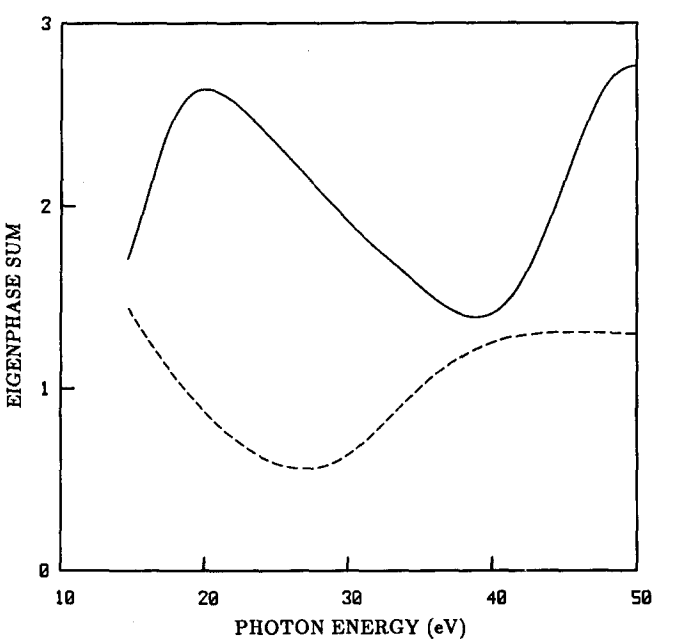

FIG. 7. Eigenphase sums for the $5\sigma_g \rightarrow k\sigma_u$ (—) and $5\sigma_g \rightarrow k\pi_u$ (---) channels.

In addition to this shape resonant behavior in the $5\sigma_g \rightarrow k\sigma_u$ continuum, the $5\sigma_g \rightarrow k\pi_u$ cross section of Fig. 6 also shows a shape resonance with a peak enhancement around 34 eV. In this region, the $k\pi_u$ eigenphase sums of Fig. 7 show an increase of about 0.75 rad. Shape resonances in other molecular systems are characterized by similar rises in the eigenphase sum. For example, a 1.25 rad increase is observed in the well-characterized $3\sigma_g \rightarrow k\sigma_u$ shape resonant partial channel in N_2.[14] In addition, this shape resonance is also associated with a broad dip in the asymmetry parameters (Fig. 8). To our knowledge, the occurrence of this shape resonance in the $5\sigma_g \rightarrow k\pi_u$ cross sections of cyanogen is unusual and has not been seen in studies of other (linear) molecules. In the K matrix associated with this resonance the $l = 3$ and 5 partial waves are strongly coupled. The $5\sigma_g \rightarrow k\pi_u$ cross sections of the multiple scattering model do not show any similar resonant enhancement. In the resulting total photoionization cross sections for the $5\sigma_g$ orbital both this π_u and the low energy σ_u shape resonances are very evident. However, the higher energy σ_u shape resonance is, as expected, obscured in the vibrationally unresolved cross sections of Fig. 6. Vibrationally resolved synchrotron radiation measurements of the cross sections in this region would be useful. In Fig. 6 we also compare our calcu-

lated $5\sigma_g$ photoionization cross sections with those of the multiple scattering model.[33] The major differences between these cross sections arise from features related to the low energy σ_u and the π_u shape resonances.

Our photoelectron asymmetry parameters for the $5\sigma_g$ level are shown in Fig. 8 along with the synchrotron radiation measurements of Holland *et al.*[32] extending up to 24 eV and the line source (Ne I, He I, and Ne II) data of Kreile *et al.*[33] Figure 8 also gives the asymmetry parameters of the multiple scattering model.[33] At low photoelectron kinetic energies the calculated and observed asymmetry parameters behave very differently. Whereas the calculated β's decrease just above threshold, the measured β's increase rapidly there. This difference may be due to autoionization which is not included in the present Hartree–Fock studies. The dip in the synchrotron radiation data and the vibrational state dependence ($\beta = 0.47$ and 0.86 for $\nu_1 = 0$ and 1, respectively) in the line source measurement at 16.85 eV are clearly due to the lower σ_u shape resonance. Our calculations predict another, but broader minimum in these asymmetry parameters around 32 eV. Unfortunately, the available synchrotron radiation data does not extend into this region. Furthermore, Fig. 8 shows the strong vibrational state dependence of β on the symmetric CN stretching (ν_1) mode seen in the line source measurement at 26.91 eV.[3] However, the calculated fixed-nuclei β value is not consistent with the observed vibrational state dependence around this energy since the intensity of the $\nu_1 = 0$ member of the $^2\Sigma_g^+ (5\sigma_g^{-1})$ band is much greater than that of the $\nu_1 = 1$ level[32,40] and hence the calculated fixed-nuclei β should be expected to be approximately equal to $\beta(\nu_1 = 0)$. Reasons for this difference are not clear. Studies of the vibrational state dependence of β on the symmetric CN stretching mode can obviously be useful here and are under way. Finally, the influence of the higher energy σ_u shape resonance on these vibrationally unresolved asymmetry parameters is not very pronounced.

In Fig. 8 we also compare the asymmetry parameters of the multiple scattering model with our present results. Although there are certainly some differences between these results, there are some important similarities.[33] For example, the influence of the two σ_u shape resonances on these β's is very evident. The minimum in β values around 23 eV is very interesting, particularly its possible correlation with the π_u shape resonance seen in our results. However, Kreile *et al.*[33] see no related resonant enhancement in the cross sections and, in fact, state that their results show no resonant behavior in the π_u channel.

C. The $B\,^2\Sigma_u^+ (4\sigma_u^{-1})$ ion

Figure 9 shows our calculated σ_g and π_g channel contributions for photoionization out of the $4\sigma_u$ level along with the corresponding total cross sections. The photon energy scale assumes an ionization potential of 14.86 eV. Figure 9 also includes results of the multiple scattering studies of Kreile *et al.*[33] The $k\sigma_g$ continuum shows the expected shape resonance enhancement in the cross section which, as discussed earlier, arises from a combination of the $l = 3$ resonances associated with the CN groups. It is interesting to note that, although this shape resonant activity is not very pronounced in the cross sections, it is very evident in both the eigenphase sums and the asymmetry parameters of Figs. 10 and 11, respectively, stressing the importance of these quantities in studies of molecular photoionization. Although there are some meaningful differences between our calculated $4\sigma_u \rightarrow k\sigma_g$ cross sections and those of multiple scattering model, this σ_g shape resonance is seen in both sets of results. However, the prominent π_g shape resonance predicted by the multiple scattering model[33] is not seen in the frozen-core Hartree–Fock (static-exchange) calculations. The behavior of our cross sections near threshold suggest that a strong discrete $4\sigma_u \rightarrow n\pi_g$ transition probably lies close to thresh-

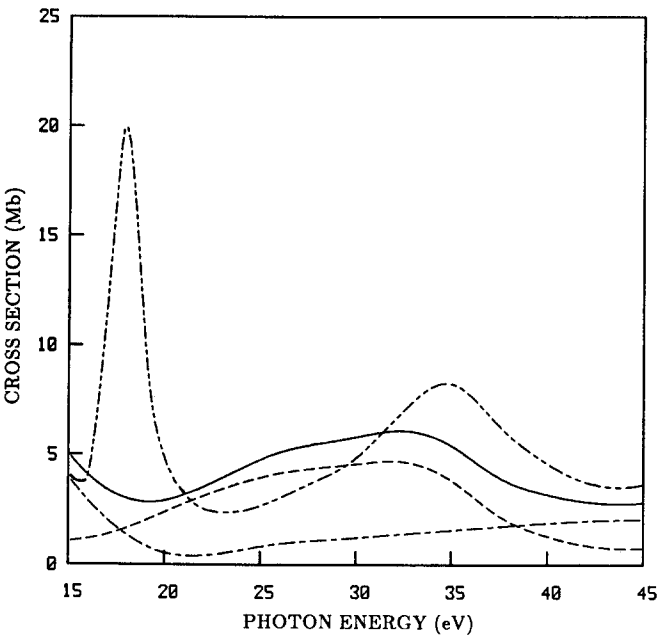

FIG. 9. Calculated photoionization cross sections for the $B\,^2\Sigma_u^+ (4\sigma_u^{-1})$ state: present results; — (total), --- ($4\sigma_u \rightarrow k\sigma_g$), and - - - ($4\sigma_u \rightarrow k\pi_g$); multiple scattering results of Ref. 33, - - - - (total).

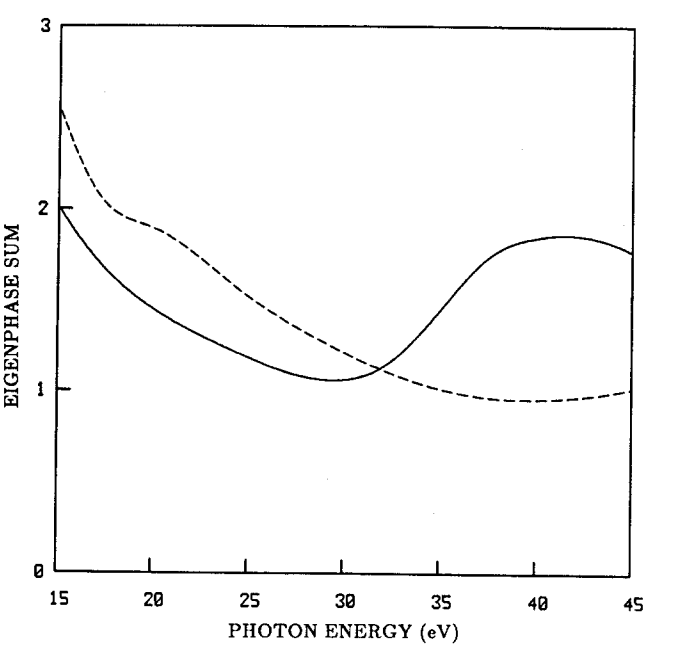

FIG. 10. Eigenphase sums for the $4\sigma_u \rightarrow k\sigma_g$ (—) and $4\sigma_u \rightarrow k\pi_g$ (---) channels.

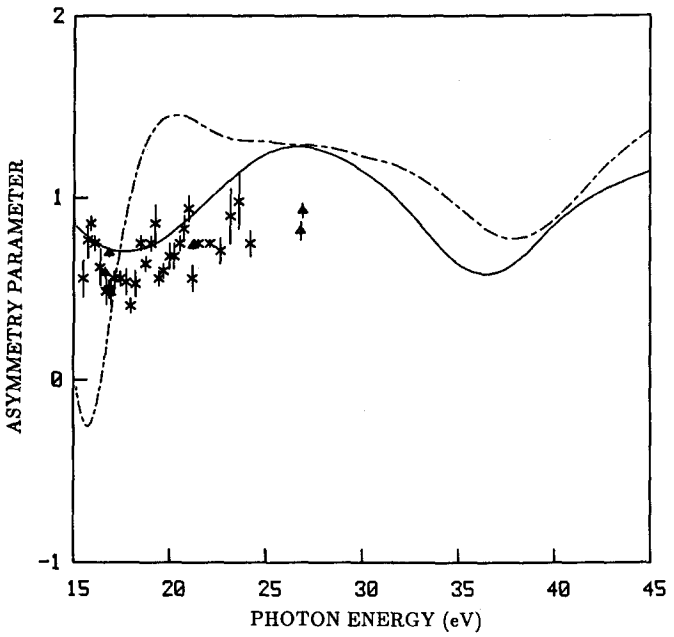

FIG. 11. Asymmetry parameter for $(4\sigma_u)^{-1}$ photoionization. See caption for Fig. 8.

old. In such a case the main difference between the Hartree–Fock and multiple scattering models is whether this $n\pi_g$ state lies below or above threshold. The actual location of this feature would be strongly influenced by electron correlation effects which could be included by one of several approaches. Synchrotron radiation measurements of the photoionization cross sections would be useful in clarifying the role of shape and autoionizing resonances in this near-threshold region.

Figure 11 shows our calculated asymmetry parameters along with the synchrotron radiation data of Holland *et al.*,[32] the line source measurements of Kreile *et al.*,[33] and the results of the multiple scattering model.[33] Some of the structure seen in these measured asymmetry parameters, e.g., around 19 eV, is clearly due to autoionization, an effect which is not included in these calculations. The calculated β's, however, are in general agreement with a background contribution implied in the measured asymmetry parameters. The σ_g shape resonance is predicted to lead to a broad minimum in the asymmetry parameters around 35 eV. Finally, there are significant differences in the values of the β's predicted by the present studies and the multiple scattering model. We also note that the differences in these calculated β's for this polyatomic system are much more substantial than seen in related studies of diatomic molecules.[14]

IV. CONCLUDING REMARKS

In this paper we have discussed the results of our studies of the photoionization cross sections and photoelectron asymmetry parameters of cyanogen using accurate Hartree–Fock electronic continuum states. The main purpose of these studies has been to extend our understanding of the dynamics of shape resonances from earlier studies of diatomic[14,26,38] and smaller polyatomic molecules[28,31] to the larger polyatomic system C_2N_2. These results do, in fact, reveal a rich shape resonant structure in the continuum of this polyatomic system with resonances in the σ_g, σ_u, and π_u symmetries. The low-energy σ_u resonance is, as expected, the C–C analog of the $l = 3$ shape resonance seen in $N_2(3\sigma_g^{-1})$ and several other diatomics. In contrast to this diatomic-like behavior, the presence of the two CN groups in C_2N_2 results in a second σ_u and a σ_g shape resonance corresponding to linear combinations of a $l = 3$ shape resonance localized on these CN sites. Moreover, our results also show a pronounced shape resonant structure in the π_u continuum. To our knowledge, such shape resonant behavior in the π_u continuum has not been seen in smaller molecular systems. Unfortunately, a comparison of these calculated photoionization cross sections and asymmetry parameters with experimental data is not presently possible since the available synchrotron radiation measurements[32] extend only up to a photon energy of 24 eV and below the energy range where many of these shape resonant features are predicted to occur in cyanogen. Finally, the agreement between the present results and those of the multiple scattering model in these studies of cyanogen is significantly less than seen in earlier studies of smaller molecular systems.[14,28]

ACKNOWLEDGMENTS

This material is based upon research supported by the National Science Foundation under Grant No. CHE-8218166. The authors acknowledge computing support from the National Center for Atmospheric Research (NCAR) which is sponsored by the National Science Foundation.

[1] J. L. Dehmer, D. Dill, and A. C. Parr, in *Photophysics and Photochemistry in the Vacuum Ultraviolet*, edited by S. McGlynn, G. Findley, and R. Huebner (Reidel, Dordrecht, Holland, 1984), pp. 341–408.
[2] V. McKoy, T. A. Carlson, and R. R. Lucchese, J. Phys. Chem. **88**, 3188 (1984).
[3] See, for example, various contributions in *Resonances in Electron–Molecule Scattering, van der Waals Complexes, and Reactive Chemical Dynamics*, ACS Symp. Ser. 263, edited by D. G. Truhlar (American Chemical Society, Washington, D.C., 1984).
[4] E. W. Plummer, T. Gustafsson, W. Gudat, and D. E. Eastman, Phys. Rev. A **15**, 2339 (1977).
[5] B. E. Cole, D. L. Ederer, R. Stockbauer, K. Codling, A. C. Parr, J. B. West, E. D. Poliakoff, and J. L. Dehmer, J. Chem. Phys. **72**, 6308 (1980).
[6] T. A. Carlson, M. O. Krause, F. A. Grimm, J. D. Allen, D. Mehaffy, P. R. Keller, and J. W. Taylor, Phys. Rev. A **23**, 3316 (1981).
[7] T. A. Carlson, M. O. Krause, F. A. Grimm, J. D. Allen, D. Mehaffy, P. R. Keller, and J. W. Taylor, J. Chem. Phys. **75**, 3288 (1981).
[8] D. M. P. Holland, J. B. West, A. C. Parr, D. L. Ederer, R. Stockbauer, R. D. Buff, and J. L. Dehmer, J. Chem. Phys. **78**, 124 (1983).
[9] P. W. Langhoff, in *Electron–Molecule and Photon–Molecule Collisions*, edited by T. N. Rescigno, B. V. McKoy, and B. Schneider (Plenum, New York, 1979).
[10] D. Dill and J. L. Dehmer, J. Chem. Phys. **61**, 692 (1974).
[11] G. Raseev, H. Le Rouzo, and H. Lefebvre-Brion, J. Chem. Phys. **72**, 5701 (1980).
[12] W. D. Robb and L. A. Collins, Phys. Rev. A **22**, 2474 (1980).
[13] B. I. Schneider and L. A. Collins, Phys. Rev. A **29**, 1695 (1984).
[14] R. R. Lucchese, G. Raseev, and V. McKoy, Phys. Rev. A **25**, 2572 (1982).
[15] M. E. Smith, V. McKoy, and R. R. Lucchese, Phys. Rev. A **29**, 1857 (1984).
[16] J. W. Davenport, Phys. Rev. Lett. **36**, 945 (1976).
[17] T. N. Rescigno, C. F. Bender, B. V. McKoy, and P. W. Langhoff, J. Chem. Phys. **68**, 970 (1978).

[18]R. R. Lucchese and V. McKoy, J. Phys. B **14**, L629 (1981).
[19]S. Wallace, D. Dill, and J. L. Dehmer, J. Phys. B **12**, L417 (1979).
[20]J. A. Stephens, D. Dill, and J. L. Dehmer, J. Phys. B **14**, 3911 (1981).
[21]N. Padial, G. Csanak, B. V. McKoy, and P. W. Langhoff, J. Chem. Phys. **69**, 2992 (1978).
[22]A. Gerwer, C. Asaro, B. V. McKoy, and P. W. Langhoff, J. Chem. Phys. **72**, 713 (1980).
[23]P. M. Dittman, D. Dill, and J. L. Dehmer, J. Chem. Phys. **76**, 5703 (1982).
[24]S. Southworth, C. M. Truesdale, P. H. Kobrin, D. W. Lindle, W. D. Brewer, and D. A Shirley, J. Chem. Phys. **76**, 143 (1982).
[25]S. Wallace, D. Dill, and J. L. Dehmer, J. Chem. Phys. **76**, 1217 (1982).
[26]M. E. Smith, R. R. Lucchese, and V. McKoy, J. Chem. Phys. **79**, 1360 (1983).
[27]J. R. Swanson, D. Dill, and J. Dehmer, J. Phys. B **14**, L207 (1981).
[28]R. R. Lucchese and V. McKoy, Phys. Rev. A **26**, 1406 (1982).
[29]F. A. Grimm, T. A. Carlson, W. B. Press, P. Agron, J. O. Thomson, and J. W. Davenport, J. Chem. Phys. **72**, 3041 (1980).
[30]L. E. Machado, E. P. Leal, G. Csanak, B. V. McKoy, and P. W. Langhoff, J. Electron Spectrosc. Relat. Phenom. **25**, 1 (1982).
[31]D. L. Lynch, M.-T. Lee, R. R. Lucchese, and V. McKoy, J. Chem. Phys. **80**, 1907 (1984).
[32]D. M. P. Holland, A. C. Parr, D. L. Ederer, J. B. West, and J. L. Dehmer, Int. J. Mass. Spectrom. Ion Phys. **52**, 195 (1983).
[33]J. Kreile, A. Schweig, and W. Thiel, Chem. Phys. Lett. **100**, 351 (1983).
[34]C. Baker and D. W. Turner, Proc. R. Soc. London Ser. A **308**, 19 (1968).
[35]R. R. Lucchese and V. McKoy, Phys. Rev. A **24**, 770 (1981).
[36]See, for example, W. H. Miller, J. Chem. Phys. **50**, 407 (1969).
[37]See, for example, T. H. Dunning, Jr. and P. J. Hay, in *Methods of Electronic Structure Theory*, edited by H. F. Schaefer III (Plenum, New York, 1977).
[38]R. R. Lucchese and V. McKoy, Phys. Rev. A **28**, 1382 (1983).
[39]A. D. McLean and M. Yoshimine, *Tables of Linear Molecular Wave Functions* (IBM Research Laboratory, San Jose, 1967), p. 218.
[40]S. Bell, Chem. Phys. Lett. **67**, 498 (1979).
[41]M. E. Smith and V. McKoy, J. Chem. Phys. **82**, 4147 (1985).